

RESEARCH PAPER

Cytotoxicity Effect of Zinc Oxide Nanoparticles and Poly-Hydroxyalkanoate)/ZnO Bionanocomposites Biosynthesis by *Lactobacillus Casei* against Breast Cancer

Zaman S. Hamza ^{1*}, Reem Jasim AL-Hendi ¹, Zahraa Nassr Jawad ¹, Nada Khazal K. Hindi ^{2,3}, Wejdan R. Tag Al- deen ⁴

¹ Biology Department, College of Science, Al-Qasim Green University, Babylon, Iraq

² Department of Basic and Medical Science, College of Nursing, Babylon University, Babylon, Iraq

³ Pharmacy College, Al-Mustaqbal University, Hillah, Iraq

⁴ Department of Biology, College of Science, University of Babylon, Al-Hilla City, Babel, Iraq

ARTICLE INFO

Article History:

Received 17 January 2025

Accepted 25 March 2025

Published 01 April 2025

Keywords:

Characterization

Cytotoxicity

Lactobacillus casei

PHA extract

ZnO/ PHA Nanobiocomposite

ABSTRACT

The process of producing zinc oxide nanoparticles using *Lactobacillus casei* and their subsequent analysis of properties. Structure and morphological measurements include research that includes measurements with X-ray diffraction, as well as the use of electron microscopy (SEM) and optical measurements. Optics measurements include UV-Vis diffusion reflection measurements and Fourier transformation infrared measurements (FTIRs). In this study, PHA was extracted from *L. casei*, and its characteristics were determined using UV spectrophotometers. The techniques used in this study are FTIR, GC-MS, DSC, and TGA. The blue Nile was used to detect PHA. In addition, the study examined the cytotoxicity of zinc oxide nanoparticles (ZnONPs) and nanobiocomposites ZnO/PHA in normal cell lines. The study found that WRL cells were exposed to ZnO extract and control substances for 24 hours at a dose of 50 to 400 ml. The biosynthesis of zinc oxide yields the lowest cell performance (72.84%), with a concentration of 400g/ml. In contrast, the Ambiguous's control group had a cell viability of 86.17 percent at the same concentration. However, the results show that WRL cells are used in the same amount of ZnO / PHA nano biocomposite extract (Z2) and ambiguous substances used as control when incubated. The ZnO/ PHA nanobiocomposite extracts have the lowest cell survival rates at 400 g/ml and have a recorded 76.20% percentage. Compared to the Ambiguous, the cell survival rate was 91.86 percent. At the same concentration, ZnO and ZnO/PHA show mild cell toxic effects in normal cells. The study studied the cytotoxic effect of ZnONPs) and nanobiocomposites (ZnO/PHA) in cancer cell lines. The results showed that MCF-7 cells were exposed to ZnO extracts at a dose of 50 to 400 mg/ml for 24 hours, with an uncertain control. Zinc oxide extraction showed the lowest MCF-7 cell viability at 400 g/ml with a percentage of 43.56 percent. In comparison, the cell viability of water-represented control groups was 79.89% at the same concentration. However, this showed that MCF-7 cells incubated at the same dose with ZnO/PHA nanocomposite extract (Z2) did not have conclusive results compared to the control. ZnO/PHA extracts have the lowest MCF-7 cell survival rate with a concentration of 400 g/ml and a percentage of 43.90%. In contrast, the same concentration of control groups treated with water had a cell survival rate of 85.24 percent. The study showed significant cytotoxicity of ZnO and ZnO/PHA on cancer cells, as opposed to normal cells.

How to cite this article

Hamza Z., AL-Hendi R., Jawad Z., Hindi N., Al- deen W. Cytotoxicity Effect of Zinc Oxide Nanoparticles and Poly-Hydroxyalkanoate)/ZnO Bionanocomposites Biosynthesis by *Lactobacillus Casei* against Breast Cancer. J Nanostruct, 2025; 15(2):446-458. DOI: 10.22052/JNS.2025.02.006

* Corresponding Author Email: zamansalman@science.uoqasim.edu.iq



INTRODUCTION

Lactic acid bacteria (LABs) and probiotic bacteria, derived from the Greek words pro and bio, respectively, play an important role in dairy technology due to their beneficial and healthy effects. When given in sufficient quantities and with strong resistance, probiotics help maintain the balance and composition of the intestinal microbes. They also increase the body's ability to resist harmful infections and protect the health of the intestine from various diseases [1, 2]. Zinc oxide nanoparticles (ZnO NPs) have chemical, physical, optical, and biological characteristics. Nanoparticles (NPs) have wide applications in many industries, including the environmental, catalyst, optical, agricultural, and biological sectors [3,4]. Zinc oxide nanoparticles (ZnONPs) are mainly used as antimicrobials for wound dressings, textiles, and food packaging [5]. Therefore, the effectiveness of ZnO nanoparticles (NPs) in inhibiting harmful germs in laboratory conditions has been evaluated against various dangerous microorganisms [6,7]. The antimicrobial effect of ZnO nanoparticles depends on their size and shape. The high volume ratio of the surface and ZnO nanoparticles improves their reactivity and, hence, their antibacterial properties [8]. Polyhydroxyalkanoates (PHAs) are highly studied and commercially used biopolymers [9]. Bacterial polyhydroxyalkanoates (PHAs) are mainly produced by bacteria as a part of the body and serve as a storage component of plants [10,11, 12].

Bionanocomposites containing different amounts of zinc oxide nanoparticles (ZnO) were created by the solution casting method using polyhydroxyalkanoates (PHA). Nanoparticles are distributed evenly throughout biopolymers without the need for surfactants or coupling agents. The nanocomposites were studied to analyze their shape, thermal characteristics, mechanical characteristics, barrier characteristics, migration characteristics, and antibacterial characteristics [13].

MATERIALS AND METHODS

Biosynthesis of ZnO Nanoparticles

Bacteria that are used in Biosynthesis

Lactobacillus casei was selected as a biological model for the synthesis of nanoparticles of ZnO from different strains, including *L. plantarium*, *L. bifidum*, *L. acidophilus*, and *L. fermentum*. It was

found that *L. casei* could synthesize and extract ZnO nanoparticles from all strains by testing all strains for the ability to produce nitric acid. It is naturally isolated from dairy products and is composed of non-pathogenic bacteria. These bacteria are identified by microscopic examination with Gram dye methods and by observing the morphology of colonies in various media and basic biochemical tests.

Synthesis of Zinc Oxide Nanoparticles by Lactobacillus casei

The biosynthesis of zinc oxide nanoparticles by *Lactobacillus casei* and the subsequent characterisation of these nanoparticles are investigated. Structure and morphological measurements encompass the X-ray diffraction measurements, scanning electron microscope (SEM), and optical measurements, including UV-Vis diffuse reflectance measurements and Fourier transform infrared (FTIR) measurements, were conducted in another study.

Extraction and quantification of PHA

A 10 mL culture was subjected to centrifugation at a speed of 5,000 revolutions per minute (rpm) for 15 minutes. The liquid portion was discarded, and the solid portion was treated with 10 mL of sodium hypochlorite. The combination was then kept at a temperature of 30 degrees Celsius for 2 hours. The combination underwent centrifugation at a speed of 5000 revolutions per minute for 15 minutes. Subsequently, it was subjected to sequential washes with distilled water, acetone, and methanol. The pellet was dissolved in 5 ml of chloroform that was heated to its boiling point. The resulting solution was then poured onto a sterile glass tray that was maintained at a temperature of 4 degrees Celsius. The solution was allowed to evaporate, and the weight of the remaining substance was measured. The relative accumulation of PHA by the several isolates was evaluated to identify the most proficient producer [14].

Characterization of PHA

The qualitative investigation of PHA involved the utilization of its chemical structure and thermal properties as criteria. The characterization and determination of native PHA-like granules required precise measurements to analyze their physical properties. In this study, five main methods were

used for characterization: infrared spectroscopy (IR), differential scanning calorimetry (DSC), thermogravimetric analysis (TGA), UV-visible spectroscopy, and gas chromatography-mass spectrometry (GC-MS).

PHA spectrophotometer assay

The polymer (PHA) extract in chloroform is transferred to a new test tube. The chloroform was volatilized and 10 ml of concentrated H₂SO₄ were introduced. The tube is sealed with a glass marble and subjected to heating for 10 minutes at a temperature of 100 °C in a water bath. After cooling, the solution is thoroughly mixed, and a portion is placed in a silica cuvette. The absorbance at 235 nm is then measured using a UV spectrophotometer with a sulfuric acid blank [15,16].

Four transform infrared Spectroscopy (FTIR)

The chloroform extract of PHA (4mg) was completely combined with KBr (Spectroscopic grade) and subjected to drying at 100°C for 4 hours. The infrared spectra of the PHA sample were captured and analyzed using a single-beam Perkin Elmer Spectrum BX series instrument from Japan. Using the given scan parameters: The scan was conducted in the range of 4000-400 cm⁻¹ with a total of 16 scans and a resolution of 4.0 cm⁻¹ [17, 18].

GC-MS analysis

A GC-MS-QP 2010 Plus model, equipped with a capillary Column-Rtx-5 MS (30 m × 0.25 mm i.d. × 0.25 μm film thickness), was used to perform a molecular analysis of pure polymer. The samples were introduced into the system using a 3 μL injection in splitless mode. The injection temperature was set at 260°C, while the column oven temperature was maintained at 100°C. The acquired mass spectra were cross-referenced with the Nist-08 and Willey-08 mass spectral collections.

Differential scanning calorimetry (DSC)

The thermal characteristics of the polymer were determined using the Pyris 1 instrument, which was connected to a cooling accessory. Before chilling at a rate of 5 C/min, the instrument was equilibrated at ambient temperature and then cooled to -40 C. A quantity of 5 milligrams of polymer was

enclosed within an aluminium pan and subjected to a temperature of approximately -40 degrees Celsius for 1 minute. The sample was then heated to a temperature of 200 degrees Celsius at a pace of 5 degrees Celsius per minute. The second chilling and heating process was conducted in the same manner, with the exception that the heating phase began at -40 °C and reached a temperature of 200 °C. The glass transition temperature (T_g) and melting temperature

(T_m) were identified based on the DSC thermogram [19].

Thermogravimetric analysis (TGA)

The thermal stability of the PHA polymer was assessed using the STA 6000 equipment manufactured by Perkin Elmer in the United States. A polymer sample weighing around 10 mg was placed in an aluminum pan and subjected to heating from around 4°C to 600°C at a rate of 10°C per minute in a nitrogen environment. This investigation was conducted to determine the decomposition temperature (T_d) of the polymer sample, which is defined as the temperature at which the sample loses 5% of its weight [20, 21].

Qualitative analysis of polyhydroxyalkanoate granules

Fluorescent Microscope

The bacterial cells were cultivated in MRS broth, then heat-fixed onto a glass slide and subsequently inundated with Nile Blue. The sample was treated with a 1% solution and incubated at 55°C for 10 minutes. Subsequently, the slide was washed with an 8% acetic acid solution for 1 minute to eliminate any remaining unstained material. The slide was flushed with tap water and then placed beneath a glass cover slip. It was then examined using a fluorescence microscope with 100x magnification and oil immersion. The microscope was equipped with cellSens® Version 1.4 Software.

Preparation of PHA films and PHA-ZnO composite films

The PHA films and PHA-ZnO composite films were prepared using the usual solvent-cast process. PHA films were fabricated by dissolving 0.3 mg of the extracted polymer in 30 ml of chloroform in a Schott bottle with magnetic stirring for 30 minutes. The resulting solution was then placed onto a glass petri dish with a diameter of 9 cm to serve as the

casting surface. The petri dishes were sealed with perforated aluminum sheets and placed in a dark location at room temperature (30 °C) for 24 hours to allow the chloroform to completely evaporate.

Solutions and Media Used in the Tissue Culture Technique

Solutions and culture Roswell Park Memorial Institute – 1640 Medium (RPMI) media used for cell culture were prepared according to [22].

The Cytotoxic Effect of Zinc Oxide Nanoparticles Synthesis from L. casei on Tumor Cell Lines

An in vitro study was conducted to examine the potential cytotoxic impact of various

concentrations of ZnO nanoparticles derived from *L. casei* on tumor cell lines (MCF-7 and A549) and a normal cell line, WRL 68.

Cell Line Maintenance

Once the cells in the vessel had formed a continuous monolayer, the subsequent according to protocol [22].

MTT Protocol

The cytotoxic effect of ZnO and ZnO/PHA nanobio composite extract from *L. casei* was performed by using an MTT ready-to-use kit (Intron Biotech).

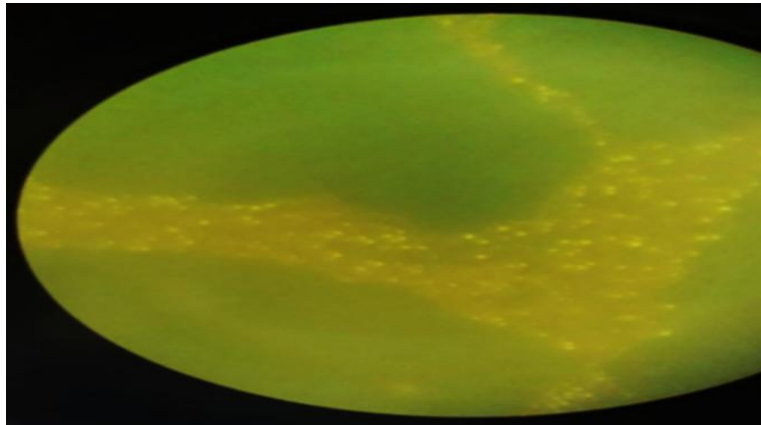


Fig. 1. *L. casei* with PHA after growth in MRS under a fluorescent microscope using Nile blue a stain at 1000x magnification.



Fig. 2. polyhydroxyalkanoate extract from *Lactobacillus casei*.

RESULTS AND DISCUSSION

Primary screening of polyhydroxyalkanoates production by Nile blue stain

The bacteria isolated from dairy starters were cultivated in the MRS broth tank and shaken for 42 hours at 36 °C. The Nile Blue A was used to quickly detect and isolate PHA-producing bacteria. Of the six isolated lactobacillus strains, only three showed positive results when dyed with a particular Nile blue colour. The PHA granules bacteria are *L. Casei*, *L. plantarum* and *L. fermentum* [23,24]. In this study, only *L. casei* was used because of its superior ability to enhance the production of PHA compared to other species. In addition, the colonies generated in the MRS media were studied under ultraviolet light (UV) to identify the pink fluorescence in Fig.

1, which acts as an indicator of the existence of the PHA producer. The user's text is empty. In blue A dye of the Nile, colonies containing PHA showed a bright orange fluorescence when exposed to UV light. As the PHA level in bacterial cells increases, the intensity of their fluorescence increases.

Extract of Polyhydroxyalkanoate by Lactobacillus bacteria

The presence of polyhydroxyalkanoate was detected in *Lactobacillus caesi*. *Lactobacilli* were kept in MRS broth for 48 hours. Cell biomass is obtained through centrifugation. The cell walls were disturbed by sodium hypochlorite. Polyhydroxyalkanoate was extracted with acetone, methanol, and chloroform. Fig. 2 shows

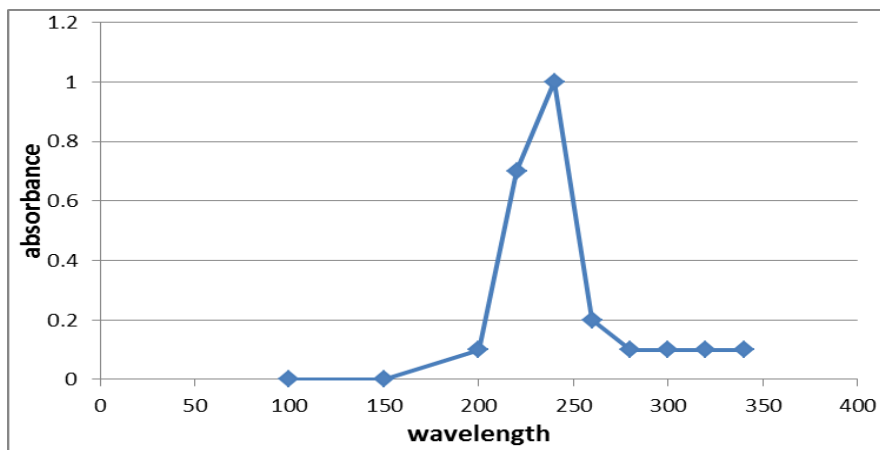


Fig. 3. UV-Vis spectrophotometer scanning spectrum of PHA compounds extracted from *Lactobacillus casei*.

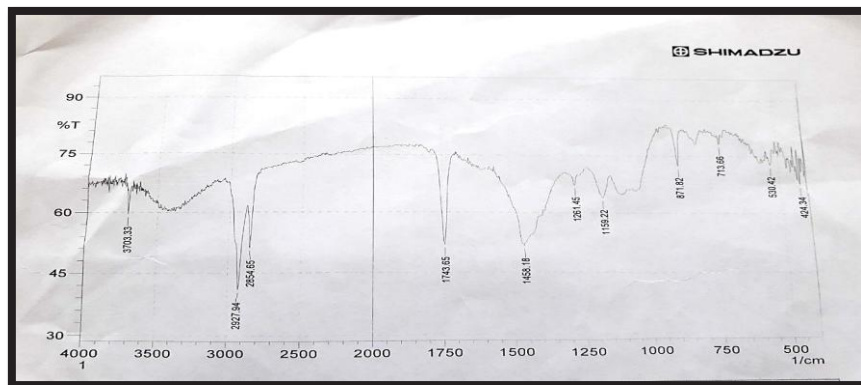


Fig. 4. FTIR of Polyhydroxyalkanoate extract from *Lactobacillus casei*.

a PHA extract from *L. Casey* observed as white powder. Studies [25] showed that when specific plasmid DNA is transferred from the bacterium to the *Escherichia coli*, the bacterium that receives it has a significant increase in PHA production. [26] stated that PHA accumulation in *Azrobacter vinelandii* UWD is related to enzyme functions of 3Kithiolase and Acetoacetyl-CoA.

Characterization of PHA extract from *Lactobacillus casei*

PHA spectrophotometer

UV-Vis scanning of the extracted polymer showed peaks at 235 nm readings extracted from *L. casei* Fig. 3. This peak range indicates the occurrence of PHA [27].

FTIR of polyhydroxyalkanoate

The extracted PHA samples were analysed using FTIR analysis to identify their functional groups (Fig. 4). Among the functional groups found are hydrogen (-OH), methyl (-CH₂), ester carbonyl

(C=O-ester), carbonyl of the amino acid protein (C=O- amino acid protein), nitrogen-hydrogen amino acid protein (N-H amino acid protein), methyl (CH₃), ether (-C-O-) and alkyl halides.

The results of the FTIR analysis showed a peak of approximately 3703 cm⁻¹ and showed that the OH terminal group formed in *Lactobacillus casei* generates a strong H bond, which is shown in Fig. 4 below. Other studies [28, 29] also reported similar results, with peaks of 2927 cm⁻¹ attributable to the expansion of the C-H bonds in the methyl and methyl groups. The results are similar to those reported in 29.30. The 1743 cm⁻¹ absorption bands correspond to the PHA marker bands assigned to the carbon C=O stretches of the ester group present in the highly organized crystal structures of the chain. The peak observed in the *Lactobacillus casei* spectrum is 1458 cm⁻¹ and corresponds to -CH₂. The highest peaks of 1261 cm⁻¹ and 1159 cm⁻¹ correspond to the existence of a -C-O bond polymer group. The presence of alkylhalides [27] indicates the extension of additional peak 871.713, 530,

Table 1. GC- Mass analysis of Polyhydroxyalkanoate extract from *Lactobacillus casei*.

No	Phytochemical name	Chemical formula	RT(min)	Molecular weight g/mol	Quality	Gas number
1	Undecanoic acid, ethyl tridecaoate	C11H22O2	11.844	186.295g/mol	90	112-37-8
		C15H30O2		242.403 g/mol	80	28267-29-0
2	Cyclohexadecane, 2-Tetradecenal 1,2- diethyle	C16H32	12.782	224.432 g/mol	53	295-65-8
		C12H26		170.34 g/mol	46	64461-99-0
3	Tetradecanoic acid	C14H28O2	14.010	228.376 g/mol	94	544-63-8
4	Oleic acid , Trans -13 octadecenoic acid	C18H34O2	16.581	282.468 g/mol	76	112-80-1
		C18H34O2		282.46 g/mol	62	112-79-8
6	Hexadecanoic acid	C16H32O2	17.715	257.422 g/mol	90	57-10-3
7	Docosane Pentatriacontane	C22H46	20.014	310.61 g/mol	96	629-97-0
		C35H72		492.961 g/mol	94	630-07-9
8	Cis-10-Nonadecenoic acid , 22-Tricosenoic acid , cycloeicosane	C19H36O2	20.459	296.495 g/mol	84	73033-09-7
		C23H44O2		352.603 g/mol	83	65119-95-1
		C12H22		166.308 g/mol	83	

and 424 cm^{-1} , and the existence of these different absorption bands proves that the polymer isolated from the lactobacillus is polyhydroxyalkanoate.

GC- MS analysis of PHA extract from *Lactobacillus casei*

GC-MS analysis helps determine the structure of the component. The main chemicals of concern were determined by analyzing their retention

peaks. In MRS media, *Lactobacillus casei* strains were grown to produce PHA containing undecanoic acid and ethyltridecaeoate. These compounds were detected at retention times of 11.844 m, with molecular weights of 186.295 g/mol and 242.403 g/mol, respectively. This information is shown in Table 1 and can also be observed in the highest form of Fig. 5. Decanoic acid is a saturated fatty acid with a straight chain of 11 carbon atoms. It

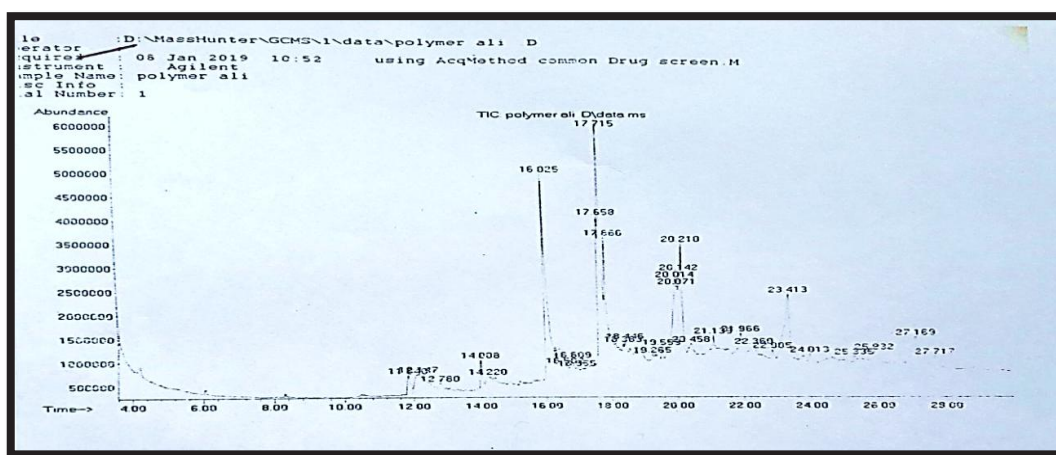


Fig. 5. GC- Mass analysis of polyhydroxyalkanoate extract from *Lactobacillus casei*.

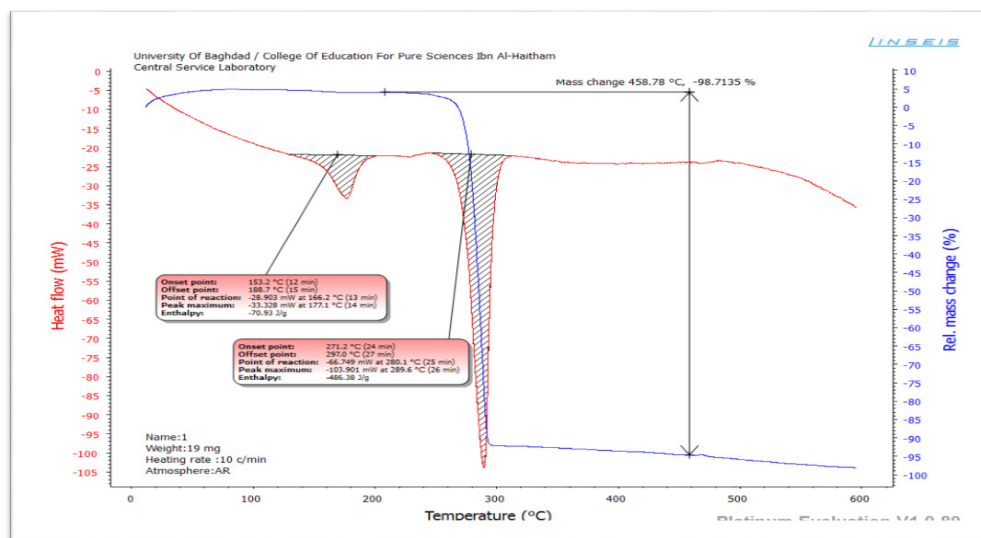


Fig. 6. Differential Scanning Calorimetry (DSC) and Thermogravimetric (TGA) of Polyhydroxyalkanoate extract from *Lactobacillus casei*.

exists in human fluids. The other related fatty acid, Tetraradiolcanoic acid, has a molecular weight of 288.376g/mol and appears at a specific time of 14.010 m. Tetradecanoic acid (also known as Myristic acid) is a 14-carbon-chain, fully saturated fatty acid. It is often found in animal and vegetable fats. A prominent peak of 3HB (hexadecanoic acid) tetramers with a molecular weight of 257,422g/mol was observed at 16.025 m and 17.715 m. Hexadecanoic acid (also known as palmitic acid) is the first synthesis fatty acid and the precursor to long fatty acids. The analysis found that monomer chains represent 21-30 percent (molecular) of the human body and belong to the biodegradable polyester family [30-32]. GC-MS analysis yielded comparable results (33). The retention period and ion fragment patterns at 20.210 min and 20.014 min are the same as those of docosane and pentatriacontane in this result, indicating the presence of random molecules. This compound is probably a product of bacterial growth in MRS enrichment media. The results are consistent with the results obtained from GC-MS analysis, as reported [34, 35].

Thermal properties of Polymer

The thermal characteristics of polyhydroxyalkanoate extracts of *Lactobacillus casei* were investigated using differential scanning calibration (DSC) and thermodynamic analysis (TGA). The results showed that the melting temperature (TM) of *L. casei*. PHA extract ranged from 153.2 °C to 188.7 °C at the initial

temperature and from 271.2 °C to 297.0 °C at the offset temperature. The findings have been documented in previous studies (section 35). TGA analysis of PHA extracted from the *Lactobacillus casei* strain was conducted to evaluate thermal stability. In Fig. 6, PHA degradation occurred in three stages. The melting point of the polymer began at 166.2 °C, indicating a process caused by the decay of the C-C atom. The second step, which occurred at 280.1 °C, corresponded to a separate reaction caused by the release of CO₂ gas. The third stage occurs at 458.78C, the point where the maximum degradation of the PHA occurs, with a mass change of 98.7135% between 166.2C and 458.78C. At 600°C, the final polymer reaction took place. Differential scanning calorimetry (DSC) analysis was carried out to examine the melting temperature, glass transition temperature, and heat associated with the melting process of PHA. PHA's melting temperature (T_m) was measured at 188.7°C, and the melting temperature for the first peak was determined at 70.93 J/g. The second peak was 297.0°C and was associated with a temperature of about 486.38J/g. These results are supported by existing literature [36].

[37] documented that the degradation of PHA occurred in two distinct phases and was fully degraded at a temperature of 300°C. In contrast, our findings demonstrate that the decomposition of PHA took place in three stages and remained intact until reaching a temperature of 320°C. However, PHA generated from *Bacillus shackletonii* K5 was destroyed in two phases, with a maximum

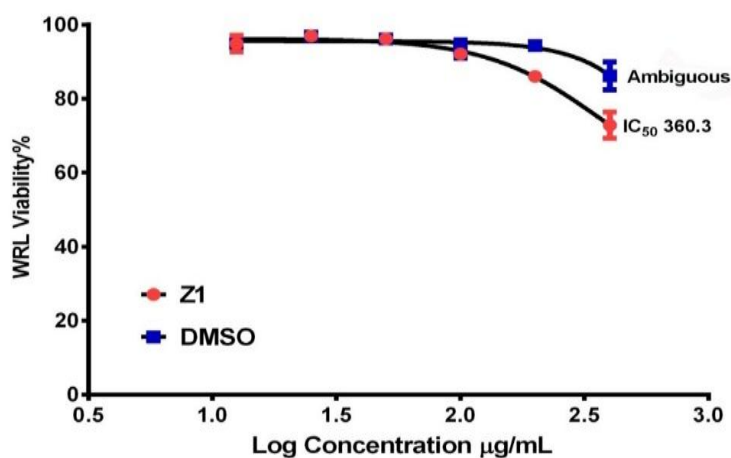


Fig. 7. Cytotoxic effect of ZnO nanoparticles extract from *L. Casei* on normal cell line.

temperature of 280°C [38].

Cytotoxic Effect of ZnO NPs (ZnONP) and ZnO/PHA Nanobiocomposite on normal cell line

The cytotoxic effect of ZnO nanoparticles and ZnO/PHA nanobiocomposite extract from Lactobacillus casei on the normal cell line (WRL) was determined using the 3-(dimethylthiazol-2-yl)-2,5-diphenyltetrazolium bromide (MTT) assay. This experiment was conducted to quantify the viability of cells and the rate of inhibition by applying various doses of Lactobacillus casei extracts on normal cell lines.

The data analysis uses a microgram per milliliter (g/ml) unit, and the logarithmic value of g/ml is plotted in GraphPad Prism 6. The diagram shows the relationship between the inhibitor concentration logarithm and the response curve. The most important IC50 values were chosen according to the best values. The viability of cells

at each time point was evaluated by colorimetric MTT tests. Table 2 shows the cytotoxicity of ZnO nanoparticles and ZnO/PHA nanobiocomposite extracts from Lactobacillus casei on normal cell lines (WRLs). The results show that certain effects were observed when WRL cells were exposed to ZnO extracts and unknown substances as controls for 24 hours at different concentrations of 50 to 400 g/ml. Cell survival is very low when compared to cancer cells depending on the dose, and the concentration of zinc oxide extract (Z1) increases. ZnO extracts have the lowest cell viability (72.84%) at 400 g/ml, while control groups (Ambiguous) have 86.17 percent cell viability at the same concentration. Since IC50 was calculated, the inhibition rate of WRL cells between zinc oxide (Z1) and control groups has not changed significantly. Zinc oxides (Z1) have the highest cytotoxic activity and have an IC50 value of 360.3 g/ml. In contrast, Ambiguous’s IC50 value is approximately 3991.

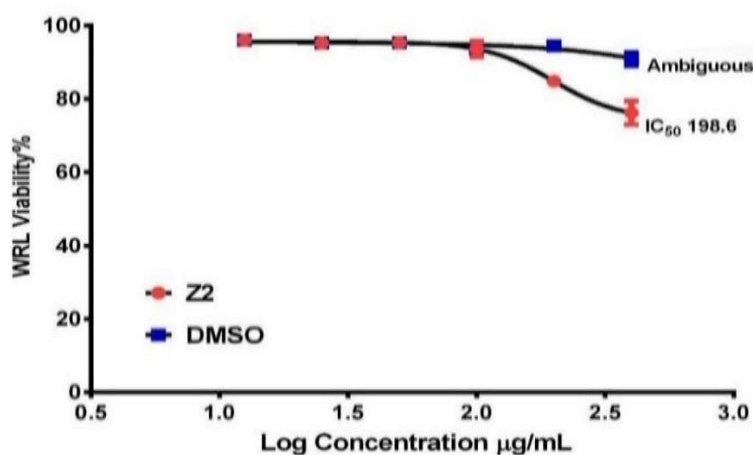


Fig. 8. Cytotoxic effect of ZnO /PHA extract from L. Casei on normal cell line.

Table 2. Cytotoxic Effect of ZnO NPs (ZnONP) and ZnO/PHA nanobiocomposite on normal cell line.

Cell line	Concentration					
	400.0	200.0	100.0	50.0	Ic50	
ZnO	Ambiguous	86.17 ±2.163	94.37±0.3983	93.46±1.403	96.18±0.7227	~ 3991
	WRL	72.84±2.028	86.03±0.4928	92.13±0.8992	96.18±0.7227	360.3
ZnO/P HA	Ambiguous	90.86±0.9979	94.47±1.213	95.33±0.6826	95.22±0.4741	~65572
	WRL	76.20±1.853	84.80±0.6955	93.60±1.212	95.33±0.6828	198.6

The result is shown in Fig. 7 [7].

However, the results of the same table show that in 24 hours of concentrations of 50 to 400 g/ml, WRL cells were incubated with ZnO/PHA nanobiocomposite extract (Z2) and unclear substances as control, and the cell's survival gradually declined depending on the dose. Cell survival decreased with the increase in the concentration of zinc oxide/PHA (Z2) extracts. ZnO/PHA nanocomposite extracts were the lowest in cell vitality (76.20%) at 400g/ml. On the contrary, in the control group Ambiguous, cell viability was 90.86% at the same concentration. IC50 calculating determined no significant changes in the inhibition rate of WRL cells between the zinc oxide/PHA nanobiocomposite and the control group. The nanobiocomposite Z2, composed of zinc oxide and PHA, showed remarkable non-cytotoxic activity, as evidenced by its IC50 value of 198.6 g/ml. This conclusion is presented in Fig. 8.

The results demonstrate that the ZnO nanoparticles and ZnO/PHA nanobiocomposite have a minimal cytotoxic effect on normal cell lines compared to cancer cells, which are significantly affected. The treatment of ZnO nanoparticles also induces the production of reactive oxygen species (ROS) in normal cells, however, the level of generation is relatively lower compared to cancer cells. This is because normal cells originally possess a lower amount of ROS and a smaller number of signaling molecules that can be transformed into more reactive species. Therefore, the oxidative stress generated may not be sufficient to induce cell death, resulting in a comparatively lesser

cytotoxic reaction. Thus, this could perhaps explain the specific ability of ZnO NPs to kill rapidly dividing cells, such as cancer cells [39, 40, 41].

Cytotoxic Effect of ZnONP) and Zno/PHA nanobiocomposite on cancer cell line

The cytotoxicity of zinc oxide nanoparticles and ZnO/PHA nanocomposite extracts of Lactobacillus casei on MCF-7 breast cancer cells was determined by 3 (dimethylthiazol-2-yl)-2,5-diphenyltetrazolium bromide (MTT) tests. This experiment is used to assess cell survival and inhibition rates by introducing different amounts of Lactobacillus casei extracts into the tumor cell lines. Data analysis is carried out using micrograms per milligram (g/ml), and the logarithmic values of g/ml are plotted using GraphPad Prism 6. This diagram is generated by plotting the logarithmic ratio of the inhibitor concentration to the response curve. The most important IC50 values were chosen based on the best values.

Table 3 shows the cytotoxic effects of ZnO nanoparticles and ZnO/PHA nanocomposite extracts from Lactobacillus casei on MCF-7 cells. The results show that MCF-7 cells are induced to decrease cell survival when exposed to ZnO extracts at concentrations of 50 to 400 g/ml for 24 hours. In other words, the cell's viability declined as the concentration of zinc oxide extract (Z1) increased. The zinc oxide extracts have the lowest MCF-7 cell activity, with a concentration of 43.56% at 400g/ml. In contrast, the Ambiguous control group cells were 79.89% of the same concentration. IC50 calculation determined the significant difference

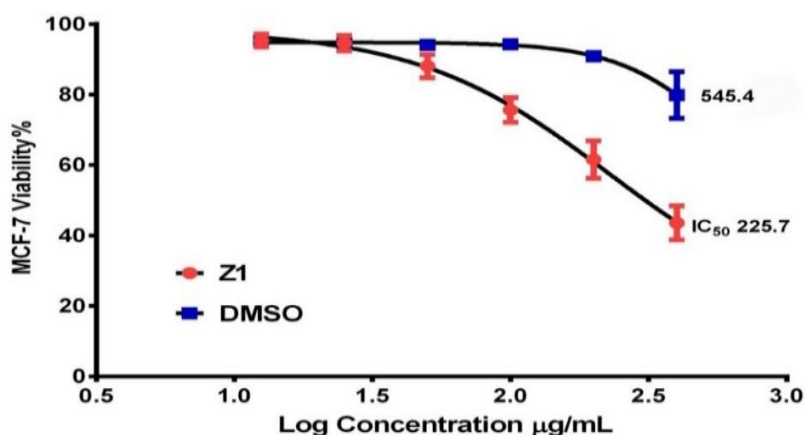


Fig. 9. Cytotoxic effect of Zno nanoparticles Extract from *L. Casei* on tumor cell line.

in MCF-7 cell inhibition rates between zinc oxide (Z1) and control groups. Zinc oxides (Z1) have the highest cell toxicity, with an IC₅₀ value of 198.6g/ml. This observation is shown in Fig. 9. However, the same table shows that the survival of MCF-7 cells decreased with dose-dependent patterns incubated for 24 hours at concentrations of 50–400 g/ml of ZnO/PHA nanocomposite (Z2). This means that the viability of cells decreases as the concentration of zinc oxides and PHA extracts (Z2) increases. Zinc oxide extraction showed the lowest growth rate of MCF-7 cells, recording 43.90% at a concentration of 400g/ml. Similarly, the control group using Ambiguous showed a cell viability of 85.24 percent at the same concentration. Significant differences in MCF-7 cell inhibition rates have been observed between zinc oxide/PHA nanobiocomposite and control groups determined by IC₅₀ calculation. The Z2 nanobiocomposite, composed of zinc oxides and PHA, has the highest toxic activity, with an IC₅₀ of 95.92g/ml. This result is shown in Fig. 10.

Multiple studies have shown that ZnONP is preferentially toxic to cancer cells, but the exact mechanism behind this selectiveness remains uncertain. ROS may explain why ZnONPs kill particularly rapidly dispersed cells. Studies show that, after treatment with ZnO nanoparticles, cancer cells produce higher levels of reactive oxygen species (ROs) than normal cells [42, 43, 44]. ROS and other signal molecules are usually rich in rapidly expanding cells, such as cancer cells, because their metabolic rate is higher than that of normal cells. Furthermore, contact with PHA nanocomposites can further strengthen the activity of these chemicals [45, 46, 47]. When cancer cells are treated with ZnO nanoparticles (NPs), the redox reaction system of nanoparticles can interact with the high levels of chemical substances and nearby signal molecules. This interaction generates additional reactive oxygen species (ROs), causing considerable oxidative stress within the cell. Finally, this oxidative stress causes cell death [48, 49, 50].

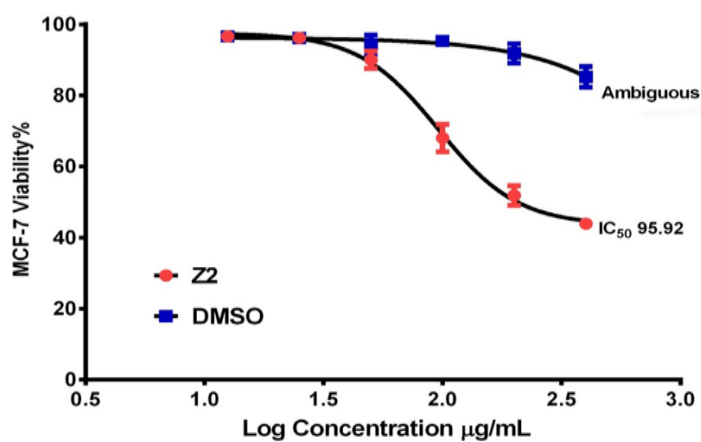


Fig. 10. Cytotoxic effect of ZnO /PHA extract from *L. casei* on tumor cell line.

Table 3. Cytotoxic Effect of ZnO NPs (ZnONP) and ZnO/PHA nanobiocomposite on cancer cell line.

Cell line		concentration				Ic50
		400.0	200.0	100.0	50.0	
ZnO	Ambiguous	79.89±3.818	90.91±0.9537	94.28±0.7561	94.08±0.7682	~65572
	MCF	43.56±2.773	61.57±3.085	75.62±2.005	88.08±1.895	198.6
ZnO/P HA	Ambiguous	85.24±1.674	91.85±1.591	95.35±0.5397	94.38±1.546	~8649
	MCF	43.90±0.8722	51.85±1.591	68.02±2.239	90.05±1.400	95.92

CONCLUSION

The current study showed that gram-positive bacteria, especially *Lactobacillus casei*, can produce polyhydroxyalkanoate (PHA) and biosynthesize zinc oxide nanoparticles. Furthermore, the biological synthesis of ZnO nanoparticles is more effective, as shown by low toxicity effects on normal cells. PHA nanofilms and their composites, including ZnO nanoparticles, showed more effective results against cancer cells than only ZnO nanoparticles.

CONFLICT OF INTEREST

The authors declare that there is no conflict of interests regarding the publication of this manuscript.

REFERENCES

1. Tripathi MK, Giri SK. Probiotic functional foods: Survival of probiotics during processing and storage. *J Funct Foods*. 2014;9:225-241.
2. Sunaryanto R, Marwoto B. ISOLASI, IDENTIFIKASI, DAN KARAKTERISASI BAKTERI ASAM LAKTAT DARI DADIH SUSU KERBAU. *Jurnal Sains dan Teknologi Indonesia*. 2013;14(3).
3. Jiang J, Pi J, Cai J. The Advancing of Zinc Oxide Nanoparticles for Biomedical Applications. *Bioinorg Chem Appl*. 2018;2018:1062562-1062562.
4. Mohd Yusof H, Mohamad R, Zaidan UH, Abdul Rahman NA. Microbial synthesis of zinc oxide nanoparticles and their potential application as an antimicrobial agent and a feed supplement in animal industry: a review. *Journal of animal science and biotechnology*. 2019;10:57-57.
5. Sirelkhatim A, Mahmud S, Seeni A, Kaus NHM, Ann LC, Bakhori SKM, et al. Review on Zinc Oxide Nanoparticles: Antibacterial Activity and Toxicity Mechanism. *Nano-micro letters*. 2015;7(3):219-242.
6. Huang Y, Mei L, Chen X, Wang Q. Recent Developments in Food Packaging Based on Nanomaterials. *Nanomaterials (Basel, Switzerland)*. 2018;8(10):830.
7. Sun Q, Li J, Le T. Zinc Oxide Nanoparticle as a Novel Class of Antifungal Agents: Current Advances and Future Perspectives. *Journal of Agricultural and Food Chemistry*. 2018;66(43):11209-11220.
8. Seil JT, Webster TJ. Antimicrobial applications of nanotechnology: methods and literature. *International journal of nanomedicine*. 2012;7:2767-2781.
9. Bugnicourt E, Cinelli P, Lazzeri A, Alvarez V. Polyhydroxyalkanoate (PHA): Review of synthesis, characteristics, processing and potential applications in packaging. *Express Polymer Letters*. 2014;8(11):791-808.
10. Marang L, van Loosdrecht MCM, Kleerebezem R. Enrichment of PHA-producing bacteria under continuous substrate supply. *N Biotechnol*. 2018;41:55-61.
11. Rodriguez-Perez S, Serrano A, Pantión AA, Alonso-Fariñas B. Challenges of scaling-up PHA production from waste streams. A review. *J Environ Manage*. 2018;205:215-230.
12. Muhammadi, Shabina, Afzal M, Hameed S. Bacterial polyhydroxyalkanoates-eco-friendly next generation plastic: Production, biocompatibility, biodegradation, physical properties and applications. *Green Chemistry Letters and Reviews*. 2015;8(3-4):56-77.
13. Díez-Pascual AM, Díez-Vicente AL. Development of Nanocomposites Reinforced with Carboxylated Poly(ether ether ketone) Grafted to Zinc Oxide with Superior Antibacterial Properties. *ACS Applied Materials & Interfaces*. 2014;6(5):3729-3741.
14. Tsado AN, Egwim EC, Oyeleke SB, Shittu OK. Screening, production and partial characterization of proteases from microbial isolates obtained from waste dumpsites. *BIOMED natural and applied science*. 2021;1(2):45-53.
15. Slepecky RA, Law JH. A Rapid Spectrophotometric Assay of Alpha, Beta-Unsaturated Acids and Beta-Hydroxy Acids. *Anal Chem*. 1960;32(12):1697-1699.
16. Kitamura S, Doi Y. Production of copolyesters from organic acids by mutant strains of *Alcaligenes eutrophus*. *Studies in Polymer Science: Elsevier*; 1994. p. 373-378.
17. Patel SKS, Kumar P, Singh M, Lee J-K, Kalia VC. Integrative approach to produce hydrogen and polyhydroxybutyrate from biowaste using defined bacterial cultures. *Bioresour Technol*. 2015;176:136-141.
18. Sathiyarayanan G, Bhatia SK, Song H-S, Jeon J-M, Kim J, Lee YK, et al. Production and characterization of medium-chain-length polyhydroxyalkanoate copolymer from Arctic psychrotrophic bacterium *Pseudomonas* sp. *PAMC 28620*. *Int J Biol Macromol*. 2017;97:710-720
19. Sabapathy PC, Devaraj S, Parthipan A, Kathirvel P. Polyhydroxyalkanoate production from statistically optimized media using rice mill effluent as sustainable substrate with an analysis on the biopolymer's degradation potential. *Int J Biol Macromol*. 2019;126:977-986.
20. Ojha N, Das N. A Statistical approach to optimize the production of Polyhydroxyalkanoates from *Wickerhamomyces anomalous* VIT-NN01 using Response Surface Methodology. *Int J Biol Macromol*. 2018;107:2157-2170.
21. Balakrishna Pillai A, Jaya Kumar A, Thulasi K, Kumarapillai H. Evaluation of short-chain-length polyhydroxyalkanoate accumulation in *Bacillus aryabhatai*. *Brazilian journal of microbiology : [publication of the Brazilian Society for Microbiology]*. 2017;48(3):451-460.
22. Freshney RI. *Culture of Animal Cells: Wiley*; 2010 2010/09/20.
23. Teeka J, Imai T, Cheng X, Reungsang A, Higuchi T, Yamamoto K, et al. Screening of PHA-Producing Bacteria Using Biodiesel-Derived Waste Glycerol as a Sole Carbon Source. *J Water Environ Technol*. 2010;8(4):373-381.
24. Kitamura S, Doi Y. Staining method of poly(3-hydroxyalkanoic acids) producing bacteria by Nile blue. *Biotechnol Tech*. 1994;8(5):345-350.
25. Lee SY, Yim KS, Chang HN, Chang YK. Construction of plasmids, estimation of plasmid stability, and use of stable plasmids for the production of poly(3-hydroxybutyric acid) by recombinant *Escherichia coli*. *J Biotechnol*. 1994;32(2):203-211.
26. Manchak J, Page WJ. Control of polyhydroxyalkanoate synthesis in *Azotobacter vinelandii* strain UWD. *Microbiology*. 1994;140(4):953-963.
27. Baskar V, Madhan R, Srinivasan G, Selvakumar K, Radha M, Rajeswari. Identifying the Potential Tetravalent Vaccine Candidate for Dengue Virus using In Silico Approach. *Insight Bioinformatics*. 2011;1(1):6-10.
28. Gumel AM, Anuar MSM, Heidelberg T. Biosynthesis and characterization of polyhydroxyalkanoates copolymers

- produced by *Pseudomonas putida* Bet001 isolated from palm oil mill effluent. *PLoS One*. 2012;7(9):e45214-e45214.
29. Bhuwal AK, Singh G, Aggarwal NK, Goyal V, Yadav A. Poly- β -hydroxybutyrate production and management of cardboard industry effluent by new *Bacillus* sp. NA10. *Bioresources and Bioprocessing*. 2014;1(1).
 30. Pachiyappan S, Ss D, Samrot AV, Kumar G N, Raj D A. Production, Optimization and Characterization of Poly[R] Hydroxyalkanoate from *Enterobacter* sp SU16. *Indian Journal of Science and Technology*. 2016;9(45).
 31. Haq lu, Tahir SF, Aftab MN, Akram F, Asad ur R, Nawaz A, et al. Purification and Characterization of a Thermostable Cellobiohydrolase from *Thermotoga petrophila*. *Protein & Peptide Letters*. 2018;25(11):1003-1014.
 32. Choi J-i, Lee SY. Process analysis and economic evaluation for Poly(3-hydroxybutyrate) production by fermentation. *Bioprocess Engineering*. 1997;17(6):335.
 33. He W, Tian W, Zhang G, Chen G-Q, Zhang Z. Production of novel polyhydroxyalkanoates by *Pseudomonas stutzeri* 1317 from glucose and soybean oil. *FEMS Microbiol Lett*. 1998;169(1):45-49.
 34. Brinda Devi A, Valli Nachiyar C. Optimization and characterization of polyhydroxyalkanoate produced by *Bacillus cereus*. *International Conference on Green technology and environmental Conservation (GTEC-2011); 2011/12: IEEE; 2011. p. 212-215.*
 35. Medvecky L. Microstructure and properties of polyhydroxybutyrate-chitosan-nanohydroxyapatite composite scaffolds. *TheScientificWorldJournal*. 2012;2012:537973-537973.
 36. Vizcaino-Caston I, Kelly CA, Fitzgerald AVL, Leeke GA, Jenkins M, Overton TW. Development of a rapid method to isolate polyhydroxyalkanoates from bacteria for screening studies. *Journal of Bioscience and Bioengineering*. 2016;121(1):101-104.
 37. Dhangdhariya JH, Dubey S, Trivedi HB, Pancha I, Bhatt JK, Dave BP, et al. Polyhydroxyalkanoate from marine *Bacillus megaterium* using CSMCRI's Dry Sea Mix as a novel growth medium. *Int J Biol Macromol*. 2015;76:254-261.
 38. Liu Y, Huang S, Zhang Y, Xu F. Isolation and characterization of a thermophilic *Bacillus shackletonii* K5 from a biotrickling filter for the production of polyhydroxybutyrate. *Journal of Environmental Sciences*. 2014;26(7):1453-1462.
 39. Steckiewicz KP, Barcinska E, Malankowska A, Zauszkiewicz-Pawlak A, Nowaczyk G, Zaleska-Medynska A, et al. Impact of gold nanoparticles shape on their cytotoxicity against human osteoblast and osteosarcoma in in vitro model. Evaluation of the safety of use and anti-cancer potential. *Journal of materials science Materials in medicine*. 2019;30(2):22-22.
 40. Lee YJ, Ahn E-Y, Park Y. Shape-dependent cytotoxicity and cellular uptake of gold nanoparticles synthesized using green tea extract. *Nanoscale research letters*. 2019;14(1):129-129.
 41. Enea M, Peixoto de Almeida M, Eaton P, Dias da Silva D, Pereira E, Soares ME, et al. A multiparametric study of gold nanoparticles cytotoxicity, internalization and permeability using an in vitro model of blood-brain barrier. Influence of size, shape and capping agent. *Nanotoxicology*. 2019;13(7):990-1004.
 42. Ostrovsky S, Kazimirsky G, Gedanken A, Brodie C. Selective cytotoxic effect of ZnO nanoparticles on glioma cells. *Nano Research*. 2009;2(11):882-890.
 43. Paino IMM, J. Gonçalves F, Souza FL, Zucolotto V. Zinc Oxide Flower-Like Nanostructures That Exhibit Enhanced Toxicology Effects in Cancer Cells. *ACS Applied Materials & Interfaces*. 2016;8(48):32699-32705.
 44. Zaman SH. Antibacterial activity of Zinc Oxide Nanoparticle (ZnONP) Biosynthesis by *Lactobacillus plantarium* against pathogenic Bacteria. *Indian Journal of Forensic Medicine & Toxicology*. 2020;14(4):2708-2715.
 45. Liou G-Y, Storz P. Reactive oxygen species in cancer. *Free radical research*. 2010;44(5):479-496.
 46. Król A, Pomastowski P, Rafińska K, Railean-Plugaru V, Buszewski B. Zinc oxide nanoparticles: Synthesis, antiseptic activity and toxicity mechanism. *Advances in Colloid and Interface Science*. 2017;249:37-52.
 47. Akhtar MJ, Ahamed M, Kumar S, Khan MM, Ahmad J, Alrokayan SA. Zinc oxide nanoparticles selectively induce apoptosis in human cancer cells through reactive oxygen species. *International journal of nanomedicine*. 2012;7:845-857.
 48. Ferrone E, Araneo R, Notargiacomo A, Pea M, Rinaldi A. ZnO Nanostructures and Electrospun ZnO-Polymeric Hybrid Nanomaterials in Biomedical, Health, and Sustainability Applications. *Nanomaterials (Basel, Switzerland)*. 2019;9(10):1449.
 49. Multiplex PCR for detection of the predominant diarrhoea-causing protozoa (*Giardia intestinalis*, *Entamoeba histolytica*, and *Cryptosporidium parvum*) in fecal samples of cattle from Babylon Province, Iraq. *Indian Journal of Forensic Medicine & Toxicology*. 2020.
 50. Kouhkan M, Ahangar P, Babaganjeh LA, Allahyari-Devin M. Biosynthesis of Copper Oxide Nanoparticles Using *Lactobacillus casei* Subsp. *Casei* and its Anticancer and Antibacterial Activities. *Current Nanoscience*. 2020;16(1):101-111.